
1-1-2001

Electron Spectral Function in Two-Dimensional Fractionalized Phases

Courtney Lannert

University of California, Santa Barbara, clannert@smith.edu

Matthew P.A. Fisher

Kavli Institute for Theoretical Physics

T. Senthil

Massachusetts Institute of Technology

Follow this and additional works at: https://scholarworks.smith.edu/phy_facpubs



Part of the [Physics Commons](#)

Recommended Citation

Lannert, Courtney; Fisher, Matthew P.A.; and Senthil, T., "Electron Spectral Function in Two-Dimensional Fractionalized Phases" (2001). Physics: Faculty Publications, Smith College, Northampton, MA. https://scholarworks.smith.edu/phy_facpubs/73

This Article has been accepted for inclusion in Physics: Faculty Publications by an authorized administrator of Smith ScholarWorks. For more information, please contact scholarworks@smith.edu

Electron spectral function in two-dimensional fractionalized phases

C. Lannert,¹ Matthew P. A. Fisher,² and T. Senthil³

¹*Department of Physics, University of California, Santa Barbara, California 93106*

²*Institute for Theoretical Physics, University of California, Santa Barbara, California 93106-4030*

³*Department of Physics, Massachusetts Institute of Technology, Cambridge, Massachusetts 02139*

(Received 16 January 2001; published 15 June 2001)

We study the electron spectral function of various zero-temperature spin-charge separated phases in two dimensions. In these phases, the electron is not a fundamental excitation of the system, but rather “decays” into a spin-1/2 chargeless fermion (the spinon) and a spinless charge e boson (the chargon). Using low-energy effective theories for the spinons (d -wave pairing plus possible Néel order) and the chargons (condensed or quantum-disordered bosons), we explore three phases of possible relevance to the cuprate superconductors: (1) AF^* , a fractionalized antiferromagnet where the spinons are paired into a state with long-ranged Néel order and the chargons are 1/2-filled and (Mott) insulating; (2) the nodal liquid, a fractionalized insulator where the spinons are d -wave paired and the chargons are uncondensed; and (3) the d -wave superconductor, where the chargons are condensed and the spinons retain a d -wave gap. Working within the Z_2 gauge theory of such fractionalized phases, our results should be valid at scales below the energy gap of the vison—the basic vortex excitation in the theory. However, on a phenomenological level, our results should apply to any spin-charge separated system where the excitations have these low-energy effective forms. Comparison with angle-resolved photoemission spectroscopy data in the undoped, pseudogapped, and superconducting regions is made.

DOI: 10.1103/PhysRevB.64.014518

PACS number(s): 74.72.–h

I. INTRODUCTION

Ideas of spin-charge separation have long been considered in relation to the cuprate high- T_c materials following Anderson’s original suggestions.¹ Phenomenologically, the assumption that the electron “breaks apart” leads to fairly simple explanations for some otherwise puzzling aspects of these materials. Attempts to formulate this rather elegant idea into a well-defined theory of electrons living in two or more spatial dimensions have historically been plagued with problems. A recently introduced Z_2 gauge theory of strongly correlated electron systems² indeed contains both spin-charge separated and spin-charge confined phases, and we work here within this formulation.

Among the host of puzzling experimental properties of these materials, we wish to concentrate here on angle-resolved photoemission spectroscopy (ARPES) experiments, which in recent years have reached an unprecedented level of resolution. With this increased clarity of data has come increased confusion in theoretical interpretation. In particular, it seems quite difficult to explain the ARPES line shape in the pseudogap regime within Fermi-liquid theory. In fact, any conventional quasiparticle description would seem to predict a sharp peak in the spectral function $A(\mathbf{k}, \omega)$ at $\omega(\mathbf{k})$ for some \mathbf{k} in the Brillouin zone. The data in the underdoped compounds in their nonsuperconducting state, on the other hand, show only broad and sometimes steplike features. Increased energy and momentum resolution has made the contrast with the superconducting state, where a sharp peak does emerge, more striking, and has led to further doubts about the quasiparticle description of the pseudogap state. As argued elsewhere,³ this contrast between the pseudogap and superconducting line shapes suggests that the pseudogap region could be dominated by a zero-temperature fractionalized phase. In addition, recent results in the superconducting

state suggest a connection between the weight under the superconducting quasiparticle peak and the condensate density.⁴ This result seems rather mysterious from a Fermi-liquid point of view, but, as we later show, may have a simple explanation in terms of separated spin and charge degrees of freedom. ARPES experiments on undoped compounds also show broad spectral features rather than well-defined quasiparticle peaks, which has led us to consider the possibility of a fractionalized antiferromagnet, dubbed AF^* . However, the spectral function does show signs of “sharpening up” as the system is overdoped, suggesting that there may be a quantum-confinement critical point in the cuprate phase diagram, as shown in Fig. 1.

We wish here to explore in more detail the consequences of these spin-charge separation ideas for the single-electron spectral function of the cuprate materials at low doping. Working with a fairly simple theory of low-energy spin and charge excitations in a fractionalized phase, we will find qualitative agreement with ARPES data in the pseudogap and superconducting phases, as well as in the undoped insulator. Although the theory used here has been analyzed and motivated from a variety of standpoints elsewhere,^{2,5} we hope to make clear its reasonableness on purely phenomeno-

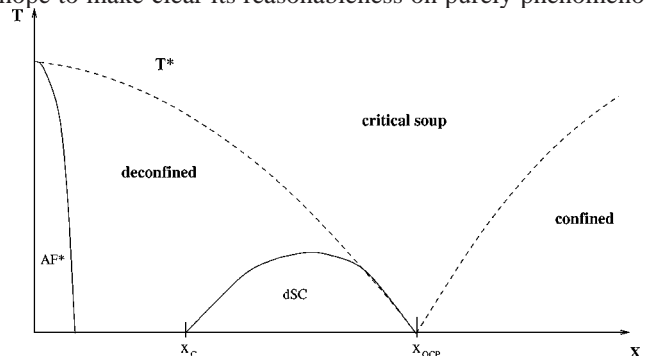


FIG. 1. Schematic phase diagram for the high- T_c cuprates.

logical grounds. We begin, then, from a zero-temperature theory of d -wave paired spinons and charge e bosons. The bosons can have a zero-temperature phase transition between condensed and quantum-disordered phases. We explore here quantitatively the single-electron spectral function in the $x=0$ spin-charge separated antiferromagnet AF^* , the nodal liquid (to be identified with the pseudogap phase), and the superconductor.

II. THE MODEL

We briefly recapitulate the phase diagram of the cuprates in terms of the Z_2 gauge theory introduced elsewhere.² The theory contains spinon and chargon degrees of freedom, coupled to a Z_2 gauge field in two spatial dimensions. We begin with the square-lattice Hamiltonian

$$\begin{aligned} H = & \sum_{\langle ij \rangle} \hat{\sigma}_{ij}^z [-t_s \hat{f}_{i\alpha}^\dagger \hat{f}_{j\alpha} + \Delta_{ij} \hat{f}_{i\uparrow} \hat{f}_{j\downarrow} - t_c \hat{b}_i^\dagger \hat{b}_j + \text{H.c.}] \\ & + U \sum_i [\hat{n}_i - (1-x)]^2 + \sum_i g \vec{N} \cdot \hat{S}_i^\pi - h \sum_{\langle ij \rangle} \hat{\sigma}_{ij}^x \\ & - K \sum_{\square} \prod_{\square} \hat{\sigma}_{ij}^z, \end{aligned} \quad (1)$$

where the electron operator is a product of spinon and chargon operators: $c_{i\alpha} = b_{i\alpha} f_{i\alpha}$. The term with coupling K is allowed by symmetry and can arise from integrating out the very-high-energy chargons, making this an effective theory of the low-energy charge degrees of freedom. The spinon pairing Δ_{ij} is taken to be d wave,

$$\Delta_{ij} = \begin{cases} +\Delta & \text{along } \hat{x} \\ -\Delta & \text{along } \hat{y}, \end{cases} \quad (2)$$

and the spin operator is $\hat{S}^\pi = \sum_k \hat{f}_{k+\pi}^\dagger \sigma \hat{f}_k$. \vec{N} is the mean-field Néel order parameter and is nonzero only within the antiferromagnetic phase. The U term is a Hubbard-like interaction for $(1-x)$ chargons per unit cell. At zero temperature and as a function of K/h , the gauge field has a transition between confining and deconfining phases.² Deep within the deconfining phase, we may set $\sigma_{ij}^z = 1$ on all links and we are left with decoupled spinons and chargons,

$$\begin{aligned} H = & \sum_{\langle ij \rangle} [-t_s \hat{f}_{i\alpha}^\dagger \hat{f}_{j\alpha} + \Delta_{ij} \hat{f}_{i\uparrow} \hat{f}_{j\downarrow} - t_c \hat{b}_i^\dagger \hat{b}_j + \text{H.c.}] \\ & + U \sum_i [\hat{n}_i - (1-x)]^2 + \sum_i \vec{N} \cdot \hat{S}_i^\pi. \end{aligned} \quad (3)$$

Fluctuations of σ^z can be taken into account by considering vortices in the Ising gauge field that have been dubbed ‘‘visons.’’ (A plaquette that contains a vison has $\prod_{\square} \sigma_{ij}^z = -1$.) The deconfining phase of the Z_2 gauge field is characterized by a gap to these vison excitations and, as we see above, the electron degrees of freedom are fractionalized in this phase. The zero-temperature confining phase of the Z_2 gauge field is a condensate of these vison excitations and

‘‘glues together’’ spinons and chargons to form electrons. A ‘‘quantum-confinement critical point’’ separates these two zero-temperature phases, as discussed elsewhere.³ At finite temperatures above the fractionalized zero-temperature phase, we expect vison excitations to exist in two dimensions, leading to interactions between the chargons and spinons. However, at temperatures much smaller than the vison gap T^{vison} (which in the simplest theories of the quantum critical point (QCP) would be of the same order as the pseudogap temperature T^*), we expect the low-energy degrees of freedom to be those of the fractionalized phase: spinons and chargons weakly interacting through Doppler shift terms, which we ignore.

We briefly discuss the phases shown pictorially in Fig. 1. In the $x_c < x < x_{QCP}$ range, starting at temperatures much less than the vison gap and lowering the temperature, the bosonic chargons should go from a phase where they are phase incoherent to one where they are condensed. Below the chargon-condensation temperature, the system is superconducting; this is T_c . Throughout, the spinons maintain a d -wave pairing (presumably due to antiferromagnetic interactions of strength J) and experience no phase transition, but rather a crossover at their pairing scale, T^* . Starting instead at zero-temperature and zero doping, we are in a spin-charge separated phase, which is also an antiferromagnetic Mott insulator with long-range Néel order. Upon increasing the doping, staying at zero temperature, we presumably enter a complicated charge-ordered insulating state of the chargons and destroy the long-range Néel order of the spinons. This is the zero-temperature phase believed to dominate the pseudogap region. We expect impurities and thermal fluctuations to destroy static charge-order, but inhomogeneous effects could still be an important high-energy presence, leading to, e.g., stripes. As the doping is further increased, the chargons presumably condense at zero temperature into a superconducting state. After the destruction of Néel order, the spinons are qualitatively the same in this doping range and maintain a d -wave gap of order T^* . Throughout this zero-temperature region, the chargons and spinons are decoupled (since we are to the left of x_{QCP}). At $x = x_{QCP}$, the Ising gauge field becomes confining and the chargons and spinons are bound together to form electrons, presumably in a Fermi-liquid phase.

We turn our attention now to the spectral function defined in terms of the electron Green function

$$A(\mathbf{k}, \omega) = -\frac{1}{\pi} \text{Im} G(\mathbf{k}, \omega). \quad (4)$$

Since at temperatures well below the vison gap, we expect a description of the system in terms of free chargons and spinons to capture the low-energy physics, we use the Hamiltonian in Eq. (3), which is a sum of spinon and chargon Hamiltonians, $H(c^\dagger, c) \simeq H_b(b^\dagger, b) + H_f(f^\dagger, f)$. Within this construction, it is possible to write the electron Green function as a product of chargon and spinon Green functions,

$$G(\mathbf{r}, \tau) = \langle T_\tau c(\mathbf{r}, \tau) c^\dagger(\mathbf{0}, 0) \rangle \quad (5)$$

$$= \langle T_\tau b(\mathbf{r}, \tau) b^\dagger(\mathbf{0}, 0) \rangle \langle T_\tau f(\mathbf{r}, \tau) f^\dagger(\mathbf{0}, 0) \rangle \quad (6)$$

$$= G_b(\mathbf{r}, \tau) G_f(\mathbf{r}, \tau), \quad (7)$$

with $\tau = it$, the imaginary time. The problem of calculating the spectral line shape in spin-charge separated phases now becomes one of calculating the spinon and chargin Green functions. We consider these two degrees of freedom in turn, discussing values of various parameters in each phase.

A. Spinons

We briefly describe the phases of the spinon model. Consider first the $\vec{N}=0$ phase that describes spinons with a d -wave pairing amplitude Δ_k . In this spin-charge separated construction, superconductivity is dependent only on the charge degrees of freedom. When the bosonic chargons are condensed ($\langle b \rangle \neq 0$), we are in a BCS d -wave superconductor and the spinons are simply neutralized BCS quasiparticles. When the chargons lack phase coherence, we are in a phase with no superconductivity, but with a d -wave gap to any excitation with spin 1/2, called elsewhere the nodal liquid.⁵ When $\vec{N} \neq 0$, spinon-antispinon pairs condense forming a state with long-range antiferromagnetic order, but still containing free-spinon excitations above a gap (of order J), which are separated from the chargons due to the vison gap. This spin-charge separated antiferromagnet has been dubbed AF^* .³

The spinon piece of the Hamiltonian in Eq. (3) is quadratic in the spinon operators, and we may diagonalize it using a Bogoliubov-type transformation. Setting $g\vec{N} = N_0\hat{z}$ and working in units of the lattice constant, we obtain

$$H_f = \sum_{\mathbf{k}} E_k \hat{a}_{k,\alpha}^\dagger \hat{a}_{k,\alpha}, \quad (8)$$

$$E_k = \sqrt{N_0^2 + \Delta_k^2 + \epsilon_k^2}, \quad (9)$$

$$\epsilon_k = -t_s(\cos k_x + \cos k_y), \quad (10)$$

$$\Delta_k = \Delta(\cos k_x - \cos k_y), \quad (11)$$

with

$$\hat{a}_{k,\alpha} = u_k \hat{d}_{k,\alpha} + \alpha v_k \hat{d}_{-k,-\alpha}^\dagger, \quad (12)$$

$$u_k^2 = \frac{1}{2} + \frac{1}{2} \cos \theta_k, \quad v_k^2 = \frac{1}{2} - \frac{1}{2} \cos \theta_k, \quad (13)$$

$$\cos \theta_k = \frac{\epsilon_k}{\sqrt{\epsilon_k^2 + \Delta_k^2}}, \quad (14)$$

where

$$\hat{d}_{k,\alpha} = A_k \hat{f}_{k,\alpha} + \alpha B_k \hat{f}_{k+\pi,\alpha}, \quad (15)$$

$$A_k^2 = \frac{1}{2} + \frac{1}{2} \cos \phi_k, \quad B_k^2 = \frac{1}{2} - \frac{1}{2} \cos \phi_k, \quad (16)$$

$$\cos \phi_k = \frac{\sqrt{\epsilon_k^2 + \Delta_k^2}}{E_k}, \quad (17)$$

is a Hartree-Fock-type spin density wave operator at momentum $\boldsymbol{\pi}$ appropriate to commensurate antiferromagnetic order with sublattice magnetization N_0 .⁶ Note that when $N_0=0$, the Hamiltonian for \hat{a}_k is the same as the effective BCS Hamiltonian for a d -wave superconductor. Indeed, when the chargons condense, these become the Bogoliubov d -wave quasiparticles.

At zero temperature, we have for the spinon correlation function,

$$\langle f_{k\alpha}^\dagger f_{k\beta} \rangle = \frac{\delta_{\alpha,\beta}}{2} \left(1 - \frac{\epsilon_k}{E_k} \right). \quad (18)$$

We see that the spinon spectrum now has a gap of N_0 at $k_x = k_y = \pi/2$, as we would expect in the Néel state, as well as a d -wave gap whose maximum is 2Δ . We expect this spinon theory to work qualitatively at all temperatures well below T^* and T^{vison} , where the spinons are strongly paired and the low-energy degrees of freedom are fractionalized. In particular, one should note that in the absence of chargin-spinon interactions, the spinons do not notice T_c .

The parameters t_s and Δ can be set by the experimentally determined ratio,

$$\frac{t_s}{\Delta} = \frac{v_f}{v_\Delta}, \quad (19)$$

which ranges from ~ 14 in YBCO ($\text{YBa}_2\text{Cu}_3\text{O}_7$) to ~ 20 in BSCCO ($\text{Bi}_2\text{Sr}_2\text{CaCu}_2\text{O}_8$) near optimal dopings.⁷ We expect this ratio to be of this order throughout the pseudogap phase. At zero doping, $|\vec{N}|$ is on the order of J .

B. Chargons

Once liberated from their fermionic statistics, the charge degrees of freedom behave as bosons of charge e hopping on a 2d square lattice, as in Eq. (3). At half-filling and zero temperature, we expect that in the limit $U/t_c \gg 1$, the system forms a Mott insulator, while in the limit $t_c/U \gg 1$, the bosons form a superfluid. This can be described by the $(2+1)$ -dimensional quantum XY model that has two phases, a superconducting phase and a quantum disordered, Mott insulating phase. Being concerned primarily with “normal state” (i.e., nonsuperconducting) properties, consider the insulating phase where $U/t_c \gg 1$. Excitations of this phase are doubly occupied sites that are “massive” (i.e., gapped) and may propagate. These excitations as well as the excitations within the superfluid phase are well described by the soft-spin continuum Landau-Ginzburg action, replacing the chargin operator with a complex field,

$$\hat{b}_i \rightarrow b(\mathbf{r}), \quad (20)$$

$$\mathcal{L}_b = \frac{1}{2} |\partial_\tau b|^2 + \frac{v^2}{2} |\nabla b|^2 + \frac{\mu}{2} |b|^2 + u(|b|^2)^2. \quad (21)$$

When $\mu > 0$, the bosons are quantum disordered and the chargin system is insulating. When $\mu < 0$, the chargons condense, forming a superconductor with $|\langle b \rangle|^2 = \mu/4u = n_0$,

where n_0 is the condensate density. Fluctuations around this new minimum are described (to quadratic order) by the action

$$b(\mathbf{r}, t) = \langle b \rangle + \tilde{b}(\mathbf{r}, t), \quad (22)$$

$$\tilde{b} = \tilde{b}_1 + i\tilde{b}_2, \quad (23)$$

$$\begin{aligned} \mathcal{L}_b = & \frac{1}{2}(\partial_t \tilde{b}_1)^2 + \frac{v^2}{2}(\nabla \tilde{b}_1)^2 + \frac{M^2}{2}(\tilde{b}_1)^2 + \frac{1}{2}(\partial_t \tilde{b}_2)^2 \\ & + \frac{v^2}{2}(\nabla \tilde{b}_2)^2, \end{aligned} \quad (24)$$

with

$$M^2 = -2\mu. \quad (25)$$

Starting in the superconducting phase and increasing the chemical potential toward $\mu=0$, the order parameter (and therefore the condensate density) vanishes at the transition.

Away from half filling in the presence of long-range Coulomb interactions or disorder, we expect the unoccupied sites to form some crystal. Even in the case of zero disorder, the underlying lattice makes characterization of this phase difficult. One way to gain intuition for this regime is by reformulating the problem in terms of vortices in the chargon phase.⁸ On physical grounds, we expect that the strong coupling of the charge degrees of freedom will lead to complicated charge-ordered states at zero temperature when the number of bosons is incommensurate with the underlying lattice, and that with increasing doping, the system should eventually pass into a zero-temperature superconducting state. The location of the transition, x_c , and the nature of the exact ground state for $x < x_c$ will depend sensitively on the chargon interactions and lattice commensurability effects. Lacking a more detailed theory of chargon solidification away from half filling in a fractionalized phase, we will use the XY model defined above to describe the low-energy degrees of freedom at low temperatures in the fractionalized phases. Our main motivation is simplicity: the (2+1)D XY model contains both a quantum-disordered and a superconducting phase of bosons, as the more correct theory of the $x > 0$ boson system should. Although this description is obviously inadequate to describe the zero-temperature phases away from half filling as well as the detailed critical properties of the transition, we note that for a perfectly clean system, the physics at length scales shorter than the mean hole spacing should be those of the half-filled system. At dopings of, say, 5% this length is about 5 lattice spacings. In the corresponding energy range, the (2+1) XY model should capture the correct physics. We note that ARPES is an intermediate energy probe, although the energies corresponding to moderate dopings may still be too high. Since we are concerned here with general features of the spectral function in each phase, we work with this phenomenological Landau-Ginzburg model, hoping to capture the correct physics.

Therefore, in the charge-disordered (nodal liquid) phase at temperatures much smaller than the vison gap, we use Eq.

(21) and find for the chargon correlation function (setting $\mu = m^2 > 0$ and ignoring u to lowest order),

$$\langle b_k^\dagger b_k \rangle = \frac{1}{\omega_k}, \quad (26)$$

$$\omega_k^2 = m^2 + v^2 |\mathbf{k}|^2. \quad (27)$$

We briefly discuss the parameters in the model, m and v . In the underdoped regime near the critical point, x_c , we expect the chargon gap to be quite small, while at half filling (in the parent insulator) the chargon gap is rather large, the charge gap for these materials being of the order of a few eV. Very little can be said about the velocity v without a more detailed microscopic theory. Working in units where \mathbf{k} is a dimensionless wavenumber, v is an energy scale and we take it to be moderately larger than the spinon kinetic scale, t_s , (but of the same order) effectively giving the charge excitations a larger bandwidth than the spinons.

In the ordered phase ($\mu < 0$), the bosons are superconducting and at $T=0$ the chargon-charge correlation function has the property

$$\lim_{\mathbf{r}' \rightarrow \mathbf{r}} \langle b^\dagger(\mathbf{r}, t) b(\mathbf{r}', t') \rangle = |\langle b \rangle|^2 = n_0, \quad (28)$$

the condensate density. The quantity $\langle b \rangle$ is precisely the order parameter of the superconductor. At dopings $x > x_c$, as temperature increases within the superfluid phase, we expect phase fluctuations to reduce this quantity, eventually causing it to vanish at $T = T_c(x)$. At zero temperature within the superfluid phase, as doping is decreased it will vanish at $x = x_c$. As discussed above, the details of the $T=0$ transition will be governed by the universality class of the true doping-dependent chargon theory.

Within the superconducting phase, we may model the bosons with Eq. (24), which results in the following general form for the chargon spectral function:

$$\langle b^\dagger(\mathbf{r}, t) b(\mathbf{r}', t') \rangle = n_0(T) + \langle \tilde{b}^\dagger(\mathbf{r}, t) \tilde{b}(\mathbf{r}', t') \rangle. \quad (29)$$

The fluctuations of the chargon field will be dominated by the detailed interactions between the chargons. In contrast to the Cooper pairs in a standard BCS superconductor, the bosonic chargons should be strongly interacting, given that their uncondensed phase is controlled by Mott-insulating physics. However, we expect that at energies larger than the condensation temperature T_c the chargon fluctuations should be the same as in the pseudogap state.

III. SPECTRAL FUNCTION

Given the spinon and chargon correlation functions, we can compute the electron spectral function, assuming no interactions between chargons and spinons, using the relations in Eqs. (4) and (5). The result at zero temperature is

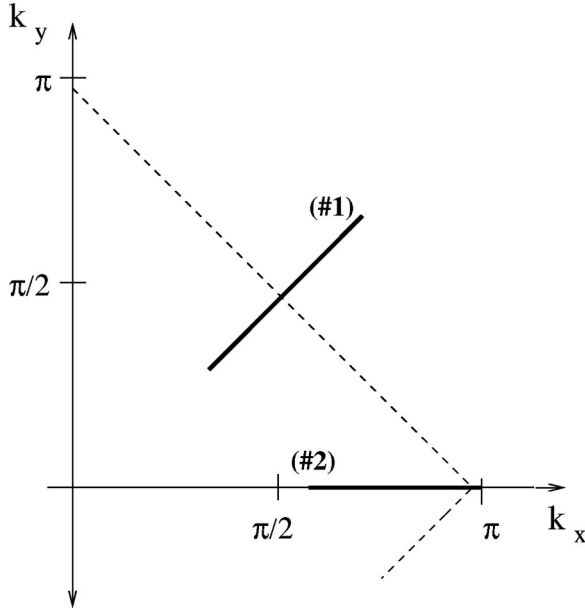


FIG. 2. Momentum cuts used for plots of $A_-(\mathbf{k}, \omega)$, showing the approximate location of the “Fermi surface” for our model. Cut No. 1 (used for MDC’s and EDC’s) is along the line $k_x = k_y$ near the nodal point, cut No. 2 (used for EDC’s) is along $k_y = 0$ near the antinodal point.

$$\begin{aligned}
 A(\mathbf{k}, \omega) &= \int_q [\langle f_q^\dagger f_q \rangle \langle b_{\mathbf{k}-q}^\dagger b_{\mathbf{k}-q} \rangle \delta(\omega - \omega_{\mathbf{k}-q} + E_q) + \langle f_q^\dagger f_q \rangle \\
 &\quad \times \langle b_{\mathbf{k}-q}^\dagger b_{\mathbf{k}-q} \rangle \delta(\omega + \omega_{\mathbf{k}-q} + E_q)], \quad (30) \\
 &= A_+(\mathbf{k}, \omega) + A_-(\mathbf{k}, \omega). \quad (31)
 \end{aligned}$$

Because it measures electrons ejected from the sample, the ARPES intensity (up to matrix elements) measures the occupied part of the spectral function, $A_-(\mathbf{k}, \omega)$.⁹ At temperatures far below the vison gap, the assumption of no chargin-spinon interactions should be valid. At energies ω larger than the temperature, the use of zero-temperature results should be valid. Most of the ARPES data of interest are done at temperatures below 100 K, which translates to an energy of 10 meV or less, close to the resolution of the instruments and certainly smaller than any features in the “normal state” spectra. This justifies use of the zero-temperature spectral function in our low-energy model. We therefore compare this $A_-(\mathbf{k}, \omega)$ with the ARPES data in each of the following phases: AF^* , nodal liquid (pseudogap), and d -wave superconductor. Although Eq. (30) is quite simple, it nevertheless is not analytically integrable for arbitrary \mathbf{k} and ω . In the following sections, we present the results of numerical integrations of this function and plot the resultant $A_-(\mathbf{k}, \omega)$ at fixed \mathbf{k} [energy distribution curve (EDC)] and at fixed ω [momentum distribution curve (MDC)], along the momentum cuts shown in Fig. 2. For the numerical integration, we approximate the delta function in Eq. (30) by a Lorentzian of small width (0.0125 eV) for the energy-distribution curves. This leads to small “tails” in these curves at small binding energies (near turnon). Since we would like to explore the momentum-distribution curves at these small turnon ener-

gies, we need to avoid measuring mostly these Lorentzian tails. To this end, for the MDC’s, we use instead a boxlike delta function,

$$\delta(x) = \begin{cases} 1/\epsilon & \text{for } -\epsilon/2 < x < \epsilon/2 \\ 0 & \text{else,} \end{cases} \quad (32)$$

with $\epsilon = 10$ meV. Values of various parameters (such as Δ and v) will be given in each section. Some “Fermi surface” properties of the spinons should be discussed. While the pairing terms technically destroy any true Fermi surface, the number of spinons at a given momentum still drops off for $\epsilon_k > 0$ and is sensitive to the minimum of the spinon dispersion, E_k , which we can call k_f . Along the (π, π) direction, this minimum occurs at $\mathbf{k} = (\pi/2, \pi/2)$, while along the $(\pi, 0)$ direction, the location of the minimum depends on the relative values of t_s and Δ and will be discussed in each phase.

A. (Fractionalized) antiferromagnet

In this phase, the spinons are particle-hole paired into an antiferromagnet (with single spinons above the gap) and the chargons are gapped into a Mott-insulating phase. However, because these two particles propagate as separate excitations, we expect an electron injected into the system to “decay” or fractionalize into these two constituents. We therefore expect the spectral function at temperatures much lower than the vison gap to be broad, without the δ function peak at some \mathbf{k} and ω which one finds when the underlying phase has electronlike elementary excitations.

For the spinons, we expect that both Δ and N_0 are of the order of $J \approx t_s/2$; we take $t_s \approx 0.5$ eV. The chargin gap m is expected to be fairly large, of the order of an eV. With this in mind, we plot the electron spectral function in Fig. 3 in the AF^* phase with $N_0 = \Delta = 0.25$ eV, $t_s = 0.5$ eV, $v = 2.5$ eV, and $m = 1$ eV. The shapes of the curves are not sensitively dependent on any of these parameters. For this ratio of t_s to Δ , the minimum of the spinon energy E_k along cut No. 2 occurs at $k_x \approx 2.2$. We plot the MDC along cut No. 1 at the energy $\omega = -1.30$ eV. This is slightly larger than the minimum binding energy of $N + m = 1.25$ eV.

A few features of these curves should be pointed out. First, all EDC’s are quite smeared with no peaks. This indeed mimics one of the features of ARPES data on the undoped compounds.¹⁰ Detailed comparison with the binding energies in the ARPES data for the undoped compound is complicated by the fact that determining the “Fermi level” of these compounds is not as straightforward as in the doped materials. In the case of our EDC plots, the binding energy should be used to note that the leading edge along cut No. 1 indeed has a smaller gap than that along cut No. 2. In fact, the difference between the two is just the factor of 2Δ . That this feature of the leading edge will track Δ_k , the d -wave gap, can be seen from Eq. (30). This is consistent with the experimentally determined “remnant Fermi surface” with a d -wave character found in the undoped compounds.¹⁰ In contrast to the EDC’s, the MDC shows a sharp feature. The detailed shape of the MDC may be influenced by the specifics of the model used.

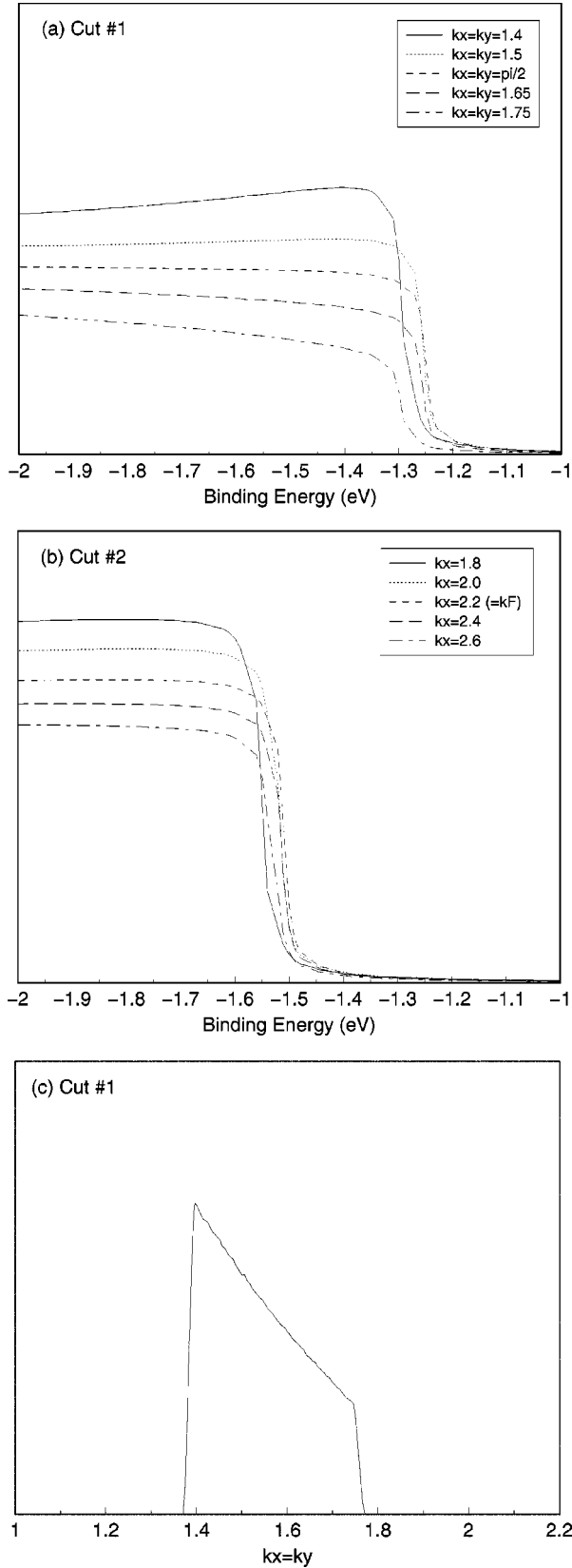


FIG. 3. $A_-(\mathbf{k}, \omega)$ at zero temperature in the AF^* phase. Plotted are: EDC's along (a) cut No. 1, and (b) cut No. 2 and an MDC (c) along cut No. 1 at energy $\omega = -1.30$ eV. The momentum space cuts are shown in Fig. 2.

B. Pseudogap (nodal liquid)

Because this zero temperature phase is also fractionalized, we expect broad spectral functions in this region. The spinons are paired into d -wave singlets, leading to the spin gap. To be precise, we calculate the spectral function at zero temperature using the XY model described earlier. We expect a low-energy theory of quantum-disordered chargons to work qualitatively for the entire pseudogap region, provided $T \ll T^{vison}$. At finite temperatures, the zero-temperature spectral function can only be expected to capture features at energies larger than T . We would therefore like to compare our spectral function in this phase with ARPES data in the underdoped compounds at $T^* \gg T > T_c$. The chargons in this region should be dominated by their zero-temperature critical point. Here, we use the critical (2+1)D XY theory for the chargons described previously, again noting that this will not describe in detail the true finite-doping critical point but will hopefully give an adequate effective theory for the low-energy excitations.

As an illustrative calculation, we may analytically perform the convolution integral in Eq. (30) for $\mathbf{k} = (\pi/2, \pi/2)$ and $\mathbf{k} = (\pi, 0)$ at small ω , exactly at the XY critical point, $m = 0$, of Eqs. (26) and (27). Eq. (30) reads

$$A_-(\mathbf{k}, \omega) = \int \frac{d^2 q}{(2\pi)^2 4\omega_q} \left(1 - \frac{\epsilon_{\mathbf{k}-\mathbf{q}}}{E_{\mathbf{k}-\mathbf{q}}} \right) \delta(\omega + E_{\mathbf{k}-\mathbf{q}} + \omega_q). \quad (33)$$

At the node, the spinon spectrum may be linearized for small momentum and we find (after rotating to momenta parallel and perpendicular to the nodal direction and setting $t_s = \Delta = \bar{v}$ for simplicity)

$$\begin{aligned} A_-[\mathbf{k} = (\pi/2, \pi/2), \omega \text{ small}] & \\ & \simeq \int \frac{d^2 q}{(2\pi)^2} \frac{1}{4vq} \left(1 - \frac{\bar{v}q_x}{\bar{v}q} \right) \delta(\omega + \bar{v}q + vq) \quad (34) \\ & \simeq \frac{1}{8\pi v} \int_0^\infty dq \delta[\omega + (v + \bar{v})q] = \frac{1}{8\pi v(v + \bar{v})} \theta(-\omega). \quad (35) \end{aligned}$$

At the antinode, the spinon spectral function is quadratic above the gap, $E_{\mathbf{k}-\mathbf{q}} \rightarrow \tilde{E}_q = 2\Delta \sqrt{1 - \frac{1}{2}q^2}$, and we find

$$\begin{aligned} A_-[\mathbf{k} = (\pi, 0), \omega \simeq \Delta] & \\ & \simeq \int \frac{d^2 q}{(2\pi)^2} \frac{1}{4vq} \left(1 + \frac{v_F[q_x^2 - q_y^2]}{2\tilde{E}_q} \right) \delta(\omega + vq + \tilde{E}_q) \quad (36) \\ & \simeq \frac{1}{8\pi v} \int_0^\infty dq \delta[\omega + vq + 2\Delta + O(q^2)] \quad (37) \\ & \simeq \frac{1}{8\pi v^2} \theta(-\omega - 2\Delta). \quad (38) \end{aligned}$$

We see that at these two particular points in \mathbf{k} space, the electron spectral function turns on like a step function, not a peak, in qualitative agreement with the ARPES results.

To obtain the electron spectral function at other \mathbf{k} and ω , we resort to numerical integration. In the underdoped region, values of t_s/Δ vary from compound to compound, but are of order ten. With this in mind, we set $t_s=0.5$ eV, $\Delta=25$ meV, and $v=2.5$ eV. Also, for the purposes of performing the integration with the Lorentzian δ function approximation (see discussion at the beginning of Sec. III), we regularize the chargon spectrum by adding a small mass, $m=12.5$ meV, for the energy distribution curves shown in Figs. 4(a) and 4(b). For the momentum distribution curve shown in Fig. 4(c), the chargon mass is equal to zero. Again, we find no sensitive dependence on the exact values of these parameters. For this value of t_s/Δ , the minimum value of the spinon energy $E_{\mathbf{k}}$ along cut No. 2 occurs at $k_x \approx 3.0$. For the MDC along cut No. 1, we use a binding energy large enough that the width of the approximate δ function does not influence the width of the curve, $\omega = -40$ meV.

We wish to note the following features of the graphs in Fig. 4. Foremost, the EDC's are indeed quite smeared, even near the ‘‘Fermi surface’’ crossings of the spinons, but more so in the $(\pi,0)$ direction than in the nodal direction, where something peakish (though still quite broad) emerges near $(\pi/2, \pi/2)$. Also, as we have seen analytically, the leading edge in the $(\pi,0)$ direction never gets to zero binding energy but instead shows a *gap* of $2\Delta=50$ meV. It should also be pointed out that as one moves along either cut, both sets of EDC's show the leading edge moving toward its minimum binding energy and then losing weight and/or receding above k_f . Of particular interest is the contrast between the EDC's and MDC along cut No. 1 (the nodal direction), where the MDC shows a very sharp peak at the node while the EDC's are broad and often steplike. The noise at the top of the MDC is a consequence of using a ‘‘boxlike’’ δ function for this integration.

C. *d*-wave superconductor

At low dopings (where $T^{vison} \gg T_c$) when we cool below T_c , the bosonic chargons develop phase coherence and $\langle b \rangle$ is nonzero. The single-electron correlation function in this region then has two pieces, in accordance with Eqs. (5) and (29)

$$G(\mathbf{r}, \tau) = |\langle b \rangle|^2 \langle f(\mathbf{r}, \tau) f^\dagger(\mathbf{0}, 0) \rangle + \langle \tilde{b}(\mathbf{r}, \tau) \tilde{b}^\dagger(\mathbf{0}, 0) \rangle \times \langle f(\mathbf{r}, \tau) f^\dagger(\mathbf{0}, 0) \rangle, \quad (39)$$

giving an occupied portion of the spectral function,

$$A_-(\mathbf{k}, \omega) = n_0(T) \langle f_{\mathbf{k}}^\dagger f_{\mathbf{k}} \rangle \delta(\omega + E_{\mathbf{k}}) + \int_{\mathbf{q}} \langle f_{\mathbf{q}}^\dagger f_{\mathbf{q}} \rangle \times \langle \tilde{b}_{\mathbf{k}-\mathbf{q}}^\dagger \tilde{b}_{\mathbf{k}-\mathbf{q}} \rangle \delta(\omega + \tilde{\omega}_{\mathbf{k}-\mathbf{q}} + E_{\mathbf{q}}). \quad (40)$$

Technically, this form is only valid at zero temperature. However, we can see from the electron Green function in Eq. (39) (which is valid at all temperatures much less than

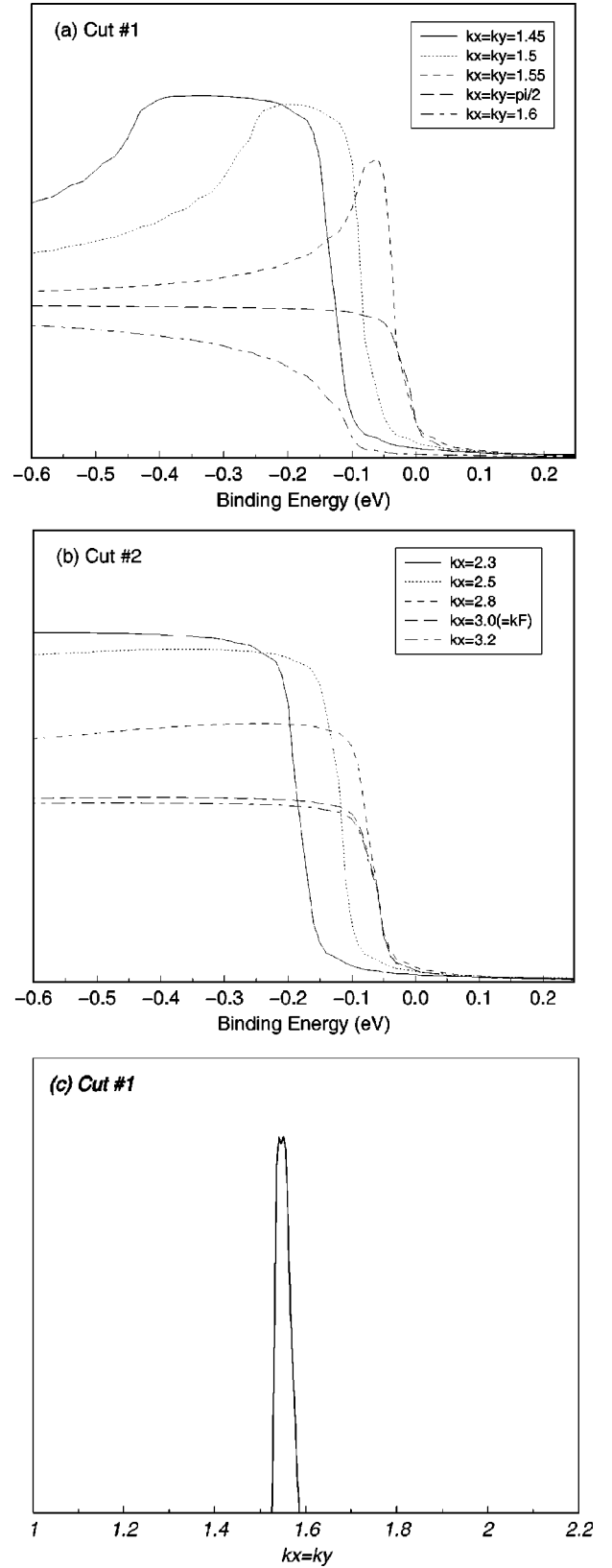


FIG. 4. $A_-(\mathbf{k}, \omega)$ in the pseudogap phase. Shown are: EDC's along (a) cut No. 1 and (b) cut No. 2 and an MDC (c) along cut No. 1 at an energy of $\omega = -40$ meV. The momentum space cuts are shown in Fig. 2.

T^{vison}) that throughout the superconducting phase at low dopings, we expect a spectral function made up of a peak and a background.

The peak is a product of the condensate density $n_0(T)$ and the spinon spectral function. For a given value of \mathbf{k} , the peak is located at the BCS quasiparticle energy E_k . Indeed, for noninteracting bosons at zero temperature, $\langle \tilde{b}^\dagger \tilde{b} \rangle = 0$, and we reproduce the BCS quasiparticle peak. In contrast with the bosons of BCS theory, we expect the chargons to be strongly interacting, leading to a nonzero background even at zero temperature.¹¹ We note that the width of this peak in our simple theory is entirely determined by the width of the spinon spectral function. Throughout the superconducting state, we expect the spinons to act like a two-dimensional Fermi liquid, leading to a weak¹² temperature-dependent width. To the extent that the peak and the background are distinguishable objects, the weight under this quasiparticle peak should be proportional to the condensate density,

$$\int_{peak} A_-(\mathbf{k}, \omega) = n_0(T) \int_{peak} \delta(\omega + E_k) = n_0(T), \quad (41)$$

and should vanish into the background as $T \rightarrow T_c$ from below, without appreciable broadening.

A comment should be made here regarding the difference between the condensate density n_0 and the superfluid stiffness ρ_s . While for noninteracting bosons these quantities are the same, for interacting bosons they are different even at zero temperature. Besides the effect of chargon-charge interactions on these quantities, there is the important effect of the Doppler-shift coupling between the superfluid and the quasiparticles in the superconducting state. For a d -wave superconductor, the coupling between quasiparticles and condensate leads to the well-known T -linear depletion of the superfluid stiffness for small T . The penetration depth, because it measures the superfluid stiffness, manifests this dependence near $T=0$. The condensate density, on the other hand, is not directly coupled to the quasiparticles and therefore need not approach $T=0$ in the same manner as the superfluid stiffness.

The background in the spectral function comes from the second term in Eq. (40) and will be complicated by the exact nature of chargon interactions. At energies large compared to the condensation temperature (≈ 10 meV), we expect the spectral function to be that of the ‘‘normal state’’ above T_c . At low energies, we have seen above that there will be a sharp (resolution-limited) peak in the spectral function, with weight equal to the condensate density, located at the spinon gap. It is only at intermediate energies (1–10 meV) that the detailed physics of the chargons at their charge-ordering critical point becomes important. In the superconductor for $T_c \ll T^{vison}$, we therefore expect a sharp peak whose weight is given by the condensate density, superimposed on a background that does not change qualitatively as one moves from

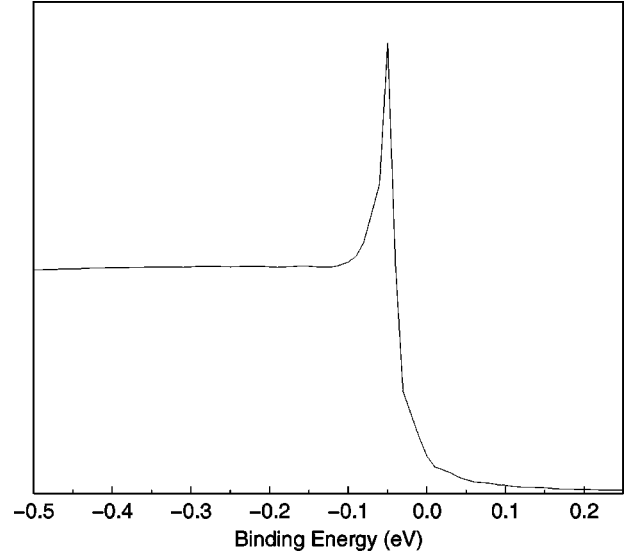


FIG. 5. For illustrative purposes only, this figure shows a Lorentzian peak centered at E_k superimposed on the nodal liquid, $A_-(\mathbf{k}, \omega)$, for the ‘‘Fermi surface’’ crossing along cut No. 2 from the previous section, $\mathbf{k} = (3.0, 0)$.

the superconductor to the pseudogap phase above T_c . An illustration of the spectral function in the superconducting phase is given in Fig. 5.

IV. CONCLUSIONS

We have shown here that the following aspects of the ARPES data in the cuprate materials can be understood by assuming spin-charge separation: (1) the d -wave ‘‘pseudogap’’ seen above T_c , (2) the lack of sharp quasiparticle peaks in the pseudogap phase, (3) the emergence of a very sharp quasiparticle peak below T_c , (4) the qualitative temperature and doping dependence of the weight under this quasiparticle peak as well as the existence within the superconducting state of a background similar in shape to the pseudogap spectra, and (5) the lack of sharp features in the undoped parent insulators as well as the d -wave character of their ‘‘remnant Fermi surface.’’ We emphasize that these results of ARPES in the undoped and underdoped compounds are rather hard to account for within a conventional picture of quasiparticles with the quantum numbers of electrons.

ACKNOWLEDGMENTS

We are grateful to Leon Balents, J.-C. Campuzano, Steve Kivelson, Doug Scalapino, and Z.-X. Shen for helpful discussions. This research was generously supported by the NSF under Grants Nos. DMR-97-04005, DMR95-28578, and PHY94-07194.

- ¹P.W. Anderson, *Science* **235**, 1196 (1987); S. Kivelson, D.S. Rokhsar, and J. Sethna, *Phys. Rev. B* **35**, 8865 (1987).
- ²T. Senthil and Matthew P.A. Fisher, *Phys. Rev. B* **62**, 7850 (2000).
- ³T. Senthil and Matthew P.A. Fisher, cond-mat/9912380 (unpublished).
- ⁴D.L. Feng, D.H. Lu, K.M. Shen, C. Kim, H. Eisaki, A. Damascelli, R. Yoshizaki, J.-i. Shimoyama, K. Kishio, G.D. Gu, S. Oh, A. Andrus, J. O'Donnel, J.N. Eckstein, and Z.-X. Shen, *Science* **289**, 277 (2000); H. Ding, J.R. Engelbrecht, Z. Wang, J.C. Campuzano, S.-C. Wang, H.-B. Yang, R. Rogan, T. Takahashi, K. Kadowaki, D.G. Hinks, cond-mat/0006143 (unpublished).
- ⁵L. Balents, M.P.A. Fisher, and C. Nayak, *Phys. Rev. B* **60**, 1654 (1999).
- ⁶G.J. Chen, Robert Joynt, F.C. Zhang, and C. Gros, *Phys. Rev. B* **42**, 2662 (1990).
- ⁷May Chiao, R.W. Hill, Christian Lupien, Louis Taillefer, P. Lambert, R. Gagnon, and P. Fournier, *Phys. Rev. B* **62**, 3554 (2000).
- ⁸The transition from superconductor to fractionalized insulator at zero-temperature can be recast through a duality transformation, in terms of the proliferation and condensation of hc/e vortices. On a lattice with $1-x$ bosons per unit cell, these vortices see $2\pi(1-x)$ flux through each plaquette. As the vortices proliferate, this flux frustrates vortex motion, which we expect to lead to spontaneous breaking of translational or rotational symmetries.
- ⁹Mohit Randeria and Juan-Carlos Campuzano, cond-mat/9709107 (unpublished).
- ¹⁰F. Ronning, C. Kim, D.L. Feng, D.S. Marshall, A.G. Loeser, L.L. Miller, J.N. Eckstein, I. Bozovic, and Z.-X. Shen, *Science* **282**, 2067 (1998).
- ¹¹A well-studied case of this is superfluid ^4He , where due to interactions, even at zero temperature the condensate density n_0 is much less than the total density n .
- ¹² T^3 for a $2d$ nodal Fermi liquid.